International Journal of Scientific Research in Engineering and Management (IJSREM)
Volume: 10 Issue: 04 | April - 2026 SJIF Rating: 8.659 ISSN: 2582-3930

Determination & Characterization of Aerodynamic Performance of the Leading Edge Tubercles of the Humpback Whales in the Aircraft Wing

Dr. Syed kashif hussain[1], Samed Saeed[2], Mohd Sajid Ahmed[3], Bushra Ramshiya[4], Shaik Zain Ahmed[5], Shaikh Khulud[6], Shree Charan[7], Syed Shah Sadaruddin[8]

[1]*HOD, Department of Aeronautical Engineering, Khaja Bandanwaz University, Kalaburagi, Karnataka, India*
[2,3]*Assistance Professor, Department of Mechanical Engineering Khaja Bandanwaz University*
[4, 5,6,7,8] *Students, Department of Aeronautical Engineering, Khaja Bandanwaz University*

Abstract - This study investigates and provides a detailed report on the effects of the leading edge sinusoidal protrusions (tubercles) on the performance of the aircraft wings. The leading edge geometry was inspired by the morphology of the Humpback whale flipper, which is a highly acrobatic species. The aim of this study is to determine and characterize the aerodynamic performance of the leading edge tubercles of the Humpback whale incorporated in the aircraft wings (business jet). The medium size business jet wing has been analyzed with the leading edge tubercles with airfoil section selected is NACA 23012. The design of the wing with leading edge tubercles has been generated using design software. The finite volume method is used to analyze the wing using Ansys Fluent solver for an angle of attack (AoA) range of 0° to 16° at low speed Reynolds number. Turbulence model SST k-ω is used to simulate steady flow over normal and tubercle wing. Few specific parameters have been varied to determine an ideal tubercle configuration for the wing in terms of improved lift performance with minimal drag penalties. The objective of the work is focusing on the basic fluid-mechanics phenomena involved to show that beneficial effects of tubercles on wing leading edge.

Key Words: *Tubercles, Passive flow control, wing performance; Post-stall improvement, Humpback, Stall delay*

1. Introduction *(Size 11, Times New roman)*

In recent years, the requirement of business jets will prioritize sustainability, advance connectivity and long range comfort with market shift towards long-range aircraft. They play crucial roles to fulfill the short range business travel in order to save time and money by reducing the waiting time of general aviation transportation. The leading-edge protuberance modifications on airfoils or wings have attracted attention as a new passive flow control technique. Among all cetaceans, the humpback whale is the one who has the higher capability to perform underwater acrobatic trajectories, in addition to the well-known ability to perform jumps out of the water (Fig-1)

Here, in this chapter we learn about the modification of the leading edge that mimics the humpback whale flipper, which is believed to significantly help the whale to execute rolls and loops under water, which have been considered to increase the lift of the wing and improve the wing stall characteristics. The morphology and arrangement of the tubercles suggest that they act as improved lift devices to control flow around the flipper and to maintain lift at a high angle of attack. Subsequently a comprehensive discussion of various engineered methods of flow control provides a context for tubercles as a flow control enables identification of specific flow manipulation techniques.

Fig- 1: Hump back-whale

The purpose of the present study is to investigate the differences between aircraft conventional wing and the wing with leading edge tubercles, at low Reynolds numbers. Force measurements show the effects of tubercles on performance characteristics such as maximum lift coefficient, stall angle and drag. Comparison of these values for conventional wing and the wing with the leading edge tubercles highlights the effects of tubercles on induced drag and tip stall. The amplitude and wavelength of the sinusoidal tubercles was also varied to determine the influence of these parameters on performance for both conventional wing and the wing with the leading edge tubercles. The improved performance is defined in terms of increased lift, reduced drag and lower noise generation. Optimum tubercle arrangements are considered and the influence of surface roughness and three-dimensional effect is also explored. In addition, alternative geometric modifications similar to tubercles are investigated and their performance characteristics are compared to those of tubercles. A further aim is to identify the mechanism by which tubercles enhance performance and to determine whether more conventional flow control devices affect the flow in a similar way.

2. Background

Fish and Battle (1995) reported that the humpback whale flipper has a wing-like, high aspect ratio plan form with rounded tubercles located along the flipper's leading edge. The morphology and arrangement of the tubercles suggest that they act as improved lift devices to control flow around the flipper and to maintain lift at a high angle of attack. Inspired by this uncommon leading edge geometry of the humpback whale flipper, Watts and Fish (2001) numerically investigated the

effect of the leading edge tubercles on the forces acting on the wings at only one angle of attack of 10° by using a panel method. They found an augmentation in lift and a reduction of drag in comparison with a smooth wing, resulting in confirming the suggestion of Fish and Battle (1995). In contrast to Watts and Fish (2001) who employed a three-dimensional panel method code to investigate a rectangular wing with and without tubercles, Milosevic et al. (2004) experimentally examined the load characteristics of a three-dimensional idealized humpback flipper in a wind tunnel. The tested models are similar in plan form geometry to the humpback whale flipper. One model had tubercles along the leading edge, while the other had no tubercles and was used as a baseline for comparison. They found that a 6% increase in the maximum lift and a 40% increase in the stall angle were achieved for the model with the tubercles. They also showed that the presence of the tubercles decreases the overall drag in the range of the angle of attack of $11° \leq \alpha \leq 18°$ This work is extended in Murray et al. (2005) to include sweep angles of 15° and 30° with similar results. Furthermore, Milosevic et al. (2007) considered the a full-span rectangular wing and experimented the effect of a leading edge tubercle on the load characteristics of a full-span rectangular wing and a semi span wing, which is based on the idealized humpback whale flipper geometry. They found that the leading edge scallop reduces lift and increases the drag of the full-span rectangular wing, while the semi-span wing produces an opposite trend. This suggests that tubercle effects may be coupled with plan form shape and Reynolds number effects.

The flow between the tubercles generates counter-rotating vortices in a sacrificed separation, which assists in energizing the flow over the tubercles. The tubercle-induced flow pattern over a wing increases the lift, delays the stall, and maintains a low drag after the stall. Previous research on the aerodynamic performance of different airfoils and tubercle geometrical arrangements has found improvement in lift and drag coefficients in the post stall region. This positive effect is useful in wind turbine applications because operating wind turbines at higher wind speeds without a stall can increase power generation. Many studies have focused only on sinusoidal and wavy protuberances. No study has explored the flow process involving airfoil selection, tubercle shape, and a geometrical modification in low Re flows. Thus, this study investigated the aerodynamic performance of several leading-edge protuberance shapes, namely sinusoidal, triangular, and slots, on two low-Re airfoils, E216 and SG6043. The amplitude (A) and wavelength (W) of protuberances were selected based on the morphological properties of the flipper of humpback whales. A numerical study was performed using the commercial CFD package ANSYS FLUENT in the angle-of-arrival (AoA) range of 0° to +20°. Turbulence was modeled using the shear stress transport (SST) k-ω model. Experimental force measurements were performed in a subsonic wind tunnel facility with a highly sensitive three-component force balance.

3. Problem Definition

Aerodynamic efficiency of an airplane wing can be improved either by increasing its lift generation tendency or by reducing the drag. Recently, Bio-inspired designs have been received greater attention for the geometric modifications of airplane wings. One of the bio-inspired designs contains sinusoidal Humpback Whale (HW) tubercles, i.e., protuberances exist at the wing leading edge (LE). The tubercles have excellent flow control characteristics at low Reynolds numbers. The present work describes the effect of tubercles on swept back wing performance at various Angle Of Attack (AoA).

4. Objectives & Scope of The Work

The present study aims investigating computationally wing geometries in which the leading edge is modified by the presence of artificial bumps (tubercles), following examples in nature (“biomimetics”). Specifically, the tubercles observed in humpback whales are considered with a special focus on easy manufacturing and performance improvements, trying to overcome the observed lift coefficient reduction before stall in comparison with a standard wing.

The work includes following tasks;

- Model an existing wing as a baseline model using CAD modeling tool.
- Perform the flow analysis on the baseline model using CFD tool (Ansys Fluent) with suitable boundary conditions.
- Modify the wing leading edge with tubercles (with minor geometry modification) such that drag force is reduced.
- Analyze the both design with numerical analysis techniques to evaluate the aerodynamic performance parameters.
- Goal is to achieve better efficiency by increase in aerodynamic efficiency.

5. Methodology

The baseline wing of business jet would be selected was the NACA series airfoil section, which has a profile resembling the cross-section of humpback whale flappers. It features a chord length (c) and a span (S). In comparison to the baseline, the modified wing includes extruded protuberances along the leading edge. These protuberances follow a cosine curve with certain periods, a wavelength (λ) of 0.59m, and peak-to-valley amplitude (A) of 0.0627m is analyzed.

6. Numerical methodology

The following subsequent section details the CAD modeling of base-line wing geometry and bio-inspired sinusoidal LE design on the sweptback wing configuration. The content in the following section serve to provide information regarding airfoil section, wing CAD model, computational domain and meshing technique (grid-independent study) used throughout the analysis.

6.1. CAD Model

The swept back wing geometry considered for the present study is medium size business jet. The wing geometric dimensions are referred with the standard design text book & available literature. The computational study has been analyzed with two cases as follows.

- Case01: Baseline wing configuration.
- Case02: Wing with leading edge tubercles.

a. Baseline Wing geometry

The baseline wing CAD model (Fig-2) and wing with leading edge tubercle has been generated using design software (Ansys Space-claim). A four digit NACA series 2412 airfoil section is

selected to generate the wing model. Wing geometric parameters are as shown in the following Table 1.

Table -1: Wing parameters

Input Parameters	Value	Unit
Wing Span	15.941	m
Wing semi-Span	7.971	m
Aspect Ratio	8.3	
Taper Ratio	0.32	
Wing Plan form area	30.62	m^2
Wing Root Chord	2.910	m
Wing Tip Chord	0.931	m
Wing MAC	2.090	m
Location of MAC along Span	3.301	m

Fig- 2 : Baseline Wing profile

b. Tubercle Wing

The selection of amplitude (A) and wavelength (λ) for tubercle wing is a critical biomimetics process aimed at improving the aerodynamic performance, especially by delaying stall, enhancing life by reducing the drag at high angle of attack. These geometric parameters governing the performance of tubercle configurations and depends on the intended operational Reynolds number (Re) and desired aerodynamic characteristics. Literature research indicates that effective tubercle geometries inspired by humpback whale flipper fall within the following dimensionless ranges:

- Non-dimensional Amplitude (A): 0.005 to 0.05c (0.5% to 5% of the wing chord)
- Wavelength: 0.1 to 0.5c (10% to 50% of wing chord length)
- Optimum ratios (amplitude to wavelength) of 0.3 to 0.4 for maximum performance improvement.

Table-2 shows the selected tubercle parameters for the wing leading edge. Baseline and modified wings are designed with NACA 23012 airfoil cross sections. The wing parameters are given in the Table-2.

Table-2: Geometric Parameters for Tubercle

Wavelength (c)	λ	0.285	
Amplitude (c)	a	0.03	
wavelength Length	λ-length	0.5956	m
Number of Planes		8.0	
Amplitude Length	a-length	0.0627	m
Scale factor		0.97	

Fig- 3 : Tubercle Wing Profile

6.2. Computational Domain

To simulate the flow over wing geometry, a three dimensional computational domain of rectangular shape (Fig-4) has been selected. The boundaries of the domain are placed far enough away from the wing so that they don't artificially interfere with flow physics. A Boolean "subtract" operation was performed between wing and CFD domain to represent the wing within the fluid domain. The wing root chord, where wing and fuselage combine each other is designated as symmetry in the domain. A CAD based technique (Body of Influence, BoI, Fig-5) was used to locally refine the mesh with specific, predefined 3D elements without subdividing the entire domain.

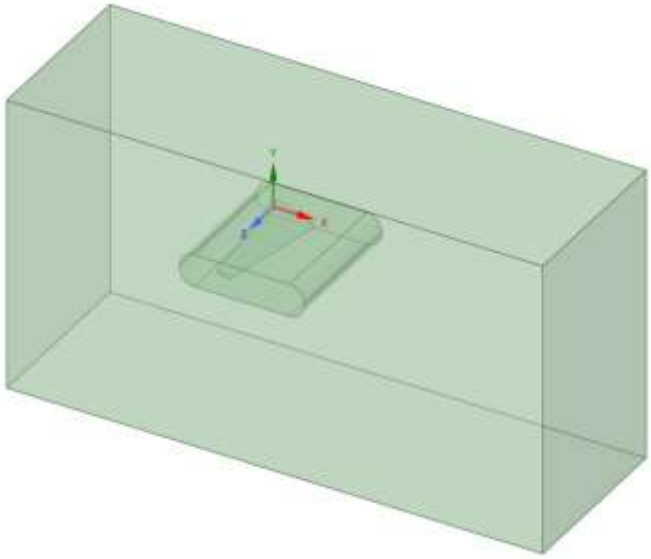

Fig- 4 : Computational Domain – Baseline Wing configuration

To achieve a fully developed flow, the total length of the computational domain with a rectangular or a C domain with unstructured and tetrahedral element mesh is used as the domain of computation. Domain is bounded by inlet at 10 chord lengths from the leading edge of wing, outlet at 15 chord lengths, far fields at 10 chord lengths on top and bottom. The total length of the computational domain is created to eliminate the reverse from the outlet boundary. The domain dimensions are given in the Table-3.

Table-3: Computational domain size

Domain Backside length	27.7	m
Domain Forward length	16.5	m
Domain Upward length	15.3	m
Domain bottom length	14.7	m
BoI length	8.4	m

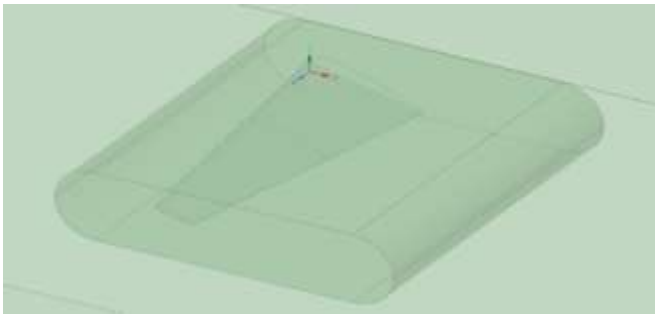

Fig- 5 : BoI – Baseline Wing configuration

6.3. Mesh/Grid Generation

The computational domain descritization (3D elements) has done using Ansys Workbench meshing tool. To capture the wing geometry an unstructured mesh with tetrahedral calls are employed in this study for all computational domain. The higher resolution of the mesh elements are generated in the region close to the wing where greater computational accuracy is needed with help of body of influence technique as shown in Fig-6 and Fig-7. The mesh refinement was done using local mesh sizing to capture the wing leading edge curvature and trailing edge closure.

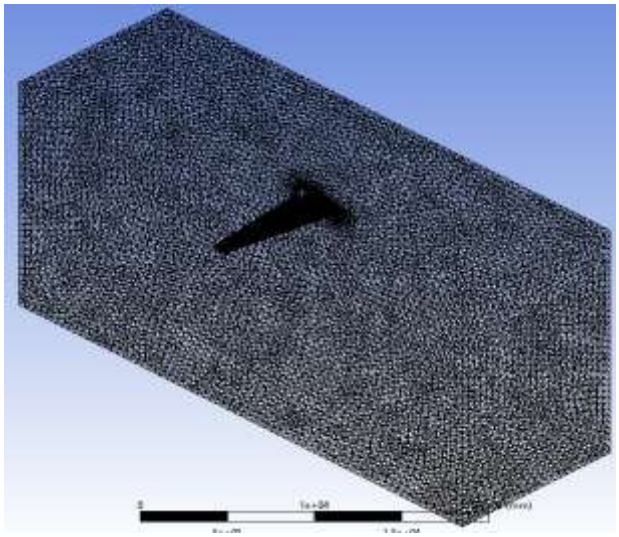

Fig- 6 : Domain Mesh

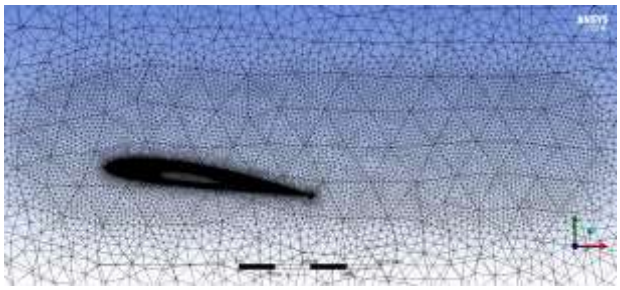

Fig- 7 : Local mesh refinement using BoI

To study the mesh sensitivity study a total of three computational meshes were generated for wing without leading-edge tubercles. Initially medium size elements are generated using local face sizing with minimum and maximum grid elements to generate total computational grid of 4.6million cells. Table-4 list-out the three grid element size carried out for angle of attack (AoA) 8 degree.

Table-4: Grid-independent study

AoA - 8 degree	Grid-01	Grid-02	Grid-03
BoI	0	64	64
Face size - 01	16	16	16
Face size - 02	16	16	16
Face size - 03	8	8	8
Min Element size	50	55	55
Max Element size	100	110	110
Growth rate	1.2	1.2	1.2
Cells per Gap	1	1	1
No. Prism layers	0	3	6
Transition Ratio	0	0.2	0.2
volume mesh	4.59M	9.4M	9.9M
Orthogonal Quality	0.15	0.201	0.173

The Fig-8 and Fig-9 shows the inflation layers generated on baseline wing to capture the transverse gradients of the fluid flow solution such as pressure and velocities within the boundary layer, same number of inflation layers are generated for the tubercle wing.

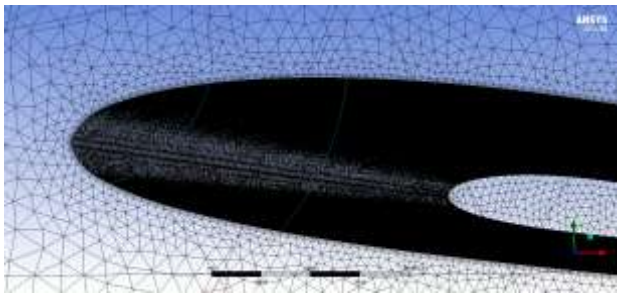

Fig- 8 : Inflation layer 01

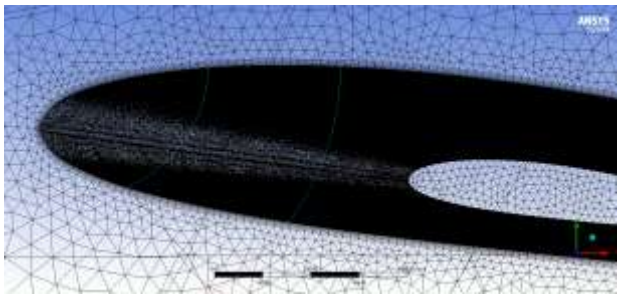

Fig- 9 : Inflation layer 02

Maximum element size of 110mm is imposed for the surfaces farthest from the model, while a sizing restriction of 8mm is generated near the wing surface. A no-slip boundary condition is imposed on the wing, whereas velocity inlet (naming selection for BC) at flow inlet, wall boundary condition at top and bottom domain boundaries, and symmetry condition at sidewalls and pressure outlet at the outlet of the domain are used. The final computational domain used in the present study is shown in Fig.-6, with six prism layers, total tetrahedral elements of 9.4 million cells with minimum orthogonal quality of 0.2. It can be clearly seen from Fig. 6 that critical areas (the leading and tailing edge of the wing) were well resolved.

7. Boundary Conditions

ANSYS Fluent solver is used to compute the flow field characteristics for baseline wing and tubercle wing profiles. The simulations are computed with an inlet velocity of 13.81m/s (U∞), resulting in a Reynolds number of 1.95x10e6 and characteristic of the normal operating conditions are considered for these types of aerial vehicles. Standard wall function applied for boundary layer simulation, while calculations carried out with two-equation turbulence model (k − ω) with a combination of Shear Stress Transport (SST) equations. The angle of attack is considered from $\alpha = 0^\circ$ to $\alpha = +16^\circ$ with a step of 4° by rotating the wing model with respect to the incident free stream velocity (U∞ - 13.81m/s) using the

same computational domain. For tubercle wing configuration, same angle of attack conditions has been studied. A total of 14 simulations are conducted excluding grid-independent study, taking a computation time approximately of 8 to 10h in each case due to the low hardware configurations.

For the convergence study, the variation in the coefficient of lift and drag values with the grid number of elements was investigated (Fig-10). The fluid properties are considered incompressible, for a free stream temperature of 300K, same as the environmental temperature in which the baseline wing and tubercle wing solutions were carried out. To solve momentum equations coupled algorithm and second order upwind special descritization is employed in the calculations. The least square cell-based method is set for spatial gradient. Residual target value of 10e−6 is set as convergence criteria

8. Results and Discussion

The computational model for the given boundary conditions provides the information on effect of tubercles for baseline wing configuration. The role of tubercles in swept back wing configuration is discussed and compared based on aerodynamic performance parameters, coefficients with baseline wing configurations.

8.1. Grid Independent Study

Grid independent study is performed for baseline wing for the AoA 8deg. The Fig-10 depicts the variation of lift and drag coefficient with respect to solution iterations. It is very clear from the graph that, lift and drag values are converged for the given flow parameters and flow boundary conditions. Residual plot indicates that after 125 solution iterations there is no change in the flow parameters. Table-5 provides the details study conducted on three grids and coefficient values.

By compare the variation of lift and drag coefficient values for the grid-02 and grid-03, the error percentage is less than two, which shows that flow parameters are independent of mesh count. Further, all solution is performed by considering the grid-02.

Table - 5: Grid Independent study

Flow Parameters	Grid-01	Grid-02	Grid-03
Inlet Velocity	13.81252	13.81252	13.81252
Hyd.Diameter	16.76535	16.76535	16.76535
MAC	2.09	2.09	2.09
Area	15.73271	15.73271	15.73271
Drag Coefficient	0.04332470	0.04289072	0.04277134
Lift Coefficient	0.80224039	0.82445921	0.82393801

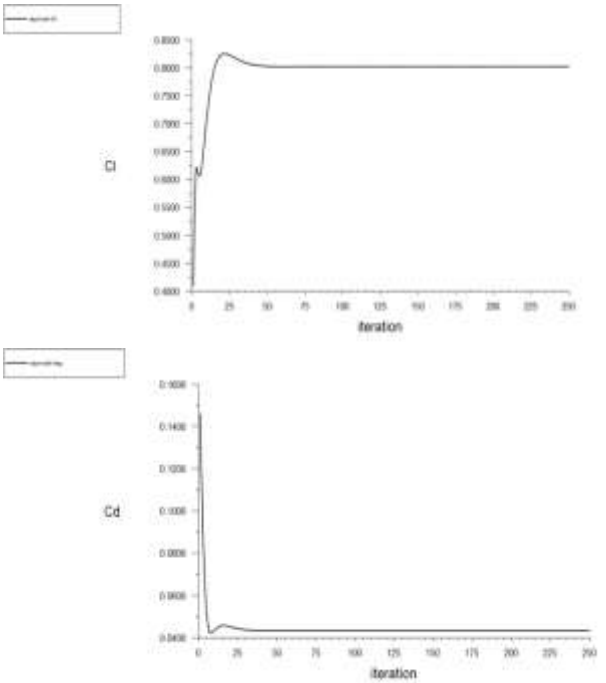

Fig- 10 : Lift and drag coefficient plot for baseline wing configuration

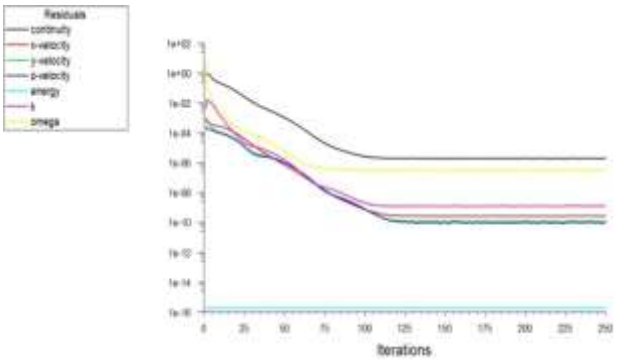

Fig- 11 : Residual plot for baseline wing configuration

8.2. Baseline Wing

The computational result for clean wing configuration (Fig. 12) depicts a linear variation of lift and drag coefficient up to AoA of 12◦ at which the maximum (C_L) is 1.074. The region after the AoA of 12◦ represents the flow transition or stall. Beyond the stall AoA, the wakes will be too large to predict. At stall, (C_D) of 0.0714 is obtained, and a drastic increment is observed thereafter as shown in the below drag coefficient plot.

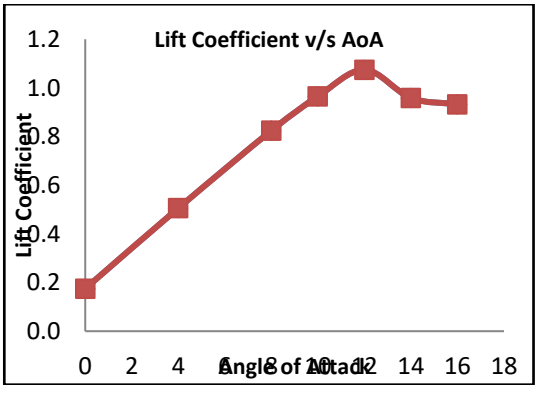

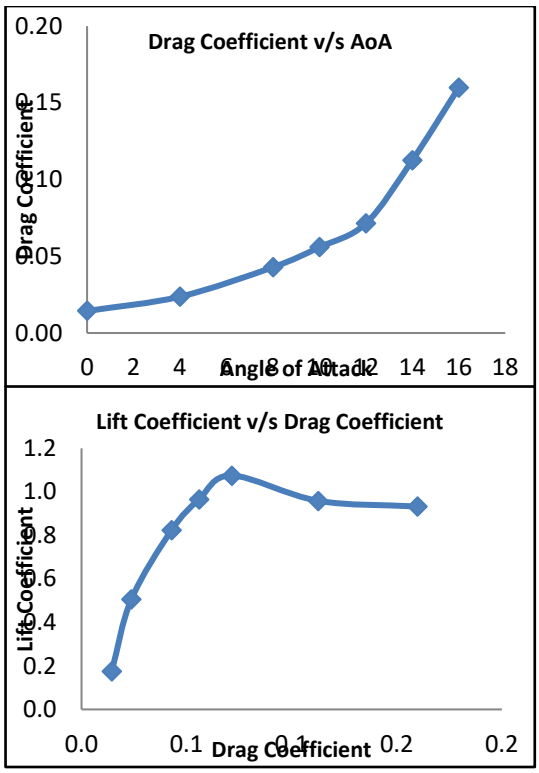

Fig- 12 : Performance Parameters-Baseline Wing

8.3. Tubercle Wing

The influence of leading edge (LE) tubercles on the wing aerodynamic characteristics (lift, drag coefficient and lift to drag ratio) of small business jet is discussed in this section. The trend in the variation of lift coefficient with AoA is similar for tubercle wing model and the baseline till AoA approximately 10deg. The tubercle wing model has slightly better performance compared to the baseline wing in post stall.

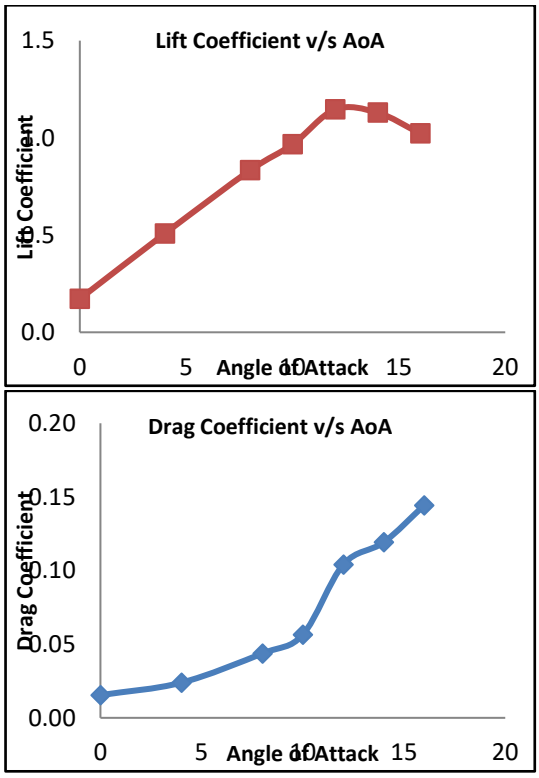

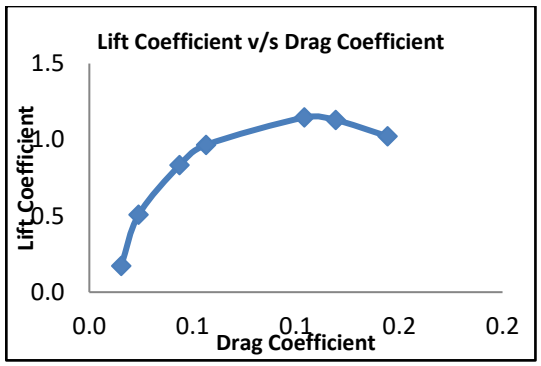

Fig- 13 : Performance Parameters - Tubercle Wing

8.4. Comparison

Fig-14 and Fig-15 shows the comparison of aerodynamic lift coefficient (C_L) and drag coefficient (C_D) at various angle of attacks (0 to 16) for a baseline unmodified wing and a tubercle wing profile. It is seen that the normal wing stalls at an angle of attack 12deg angle of attack achieving a maximum lift coefficient of 1.074. Baseline wing configurations show a linear increase in the lift coefficient with angles of attack. Beyond 12 degree the lift is decreased drastically showing a steep stall characteristic with flow separation as shown in the Fig-14. However for a tubercle wing even after 12deg angle of attack, lift is reducing gradually showing the soft stall behavior, flow separation n this case is gradual. In the drag coefficient (C_D) it is seen that tubercle has no effect at very small angle of attack (0 and 10 degree) but in the pre-stall region decreases the drag providing the better efficiency. It can be said that the tubercle wing has superior aerodynamic characteristics in the post stall region compared to normal wing profile.

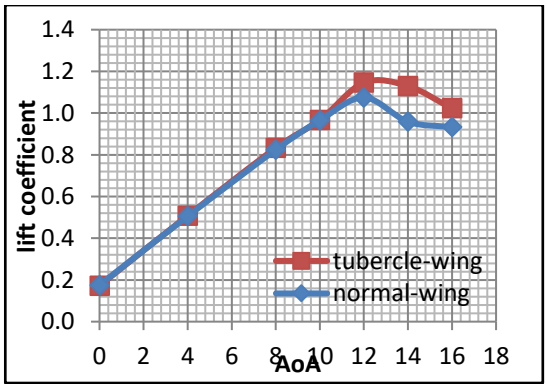

Fig- 14 : Lift Curve slope comparison

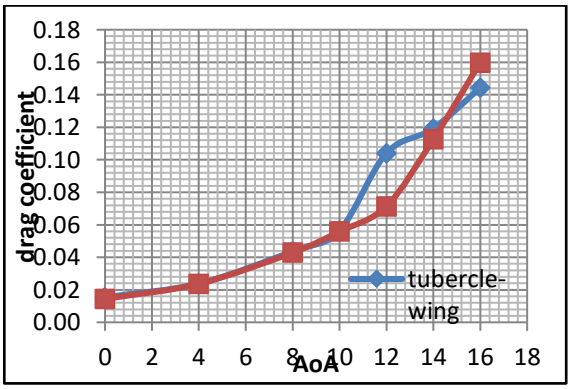

Fig- 15 : Drag slope comparison

As it is indicated from the lift curve slope, the variation of lift coefficient with AoA is linear up to 10deg angle of attack; hence CFD post has been carried out for higher AoA showing the advantages of leading edge tubercle over baseline wing. Fig-14 to Fig-31 shows the velocity contours, streamline and velocity vectors comparison for both wing designs for 14deg and 16deg angle of attack.

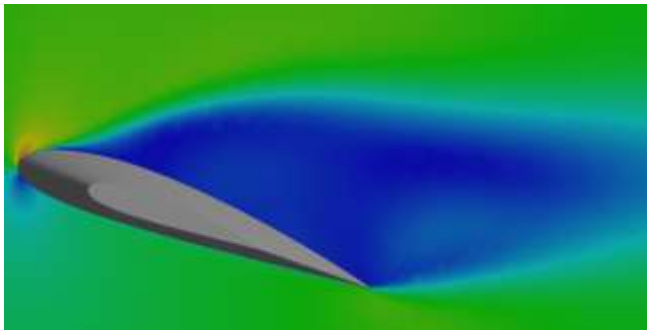

Fig- 16 : Velocity contours @ 14deg AoA – Spanwise section (4m from root chord) view for basic wing

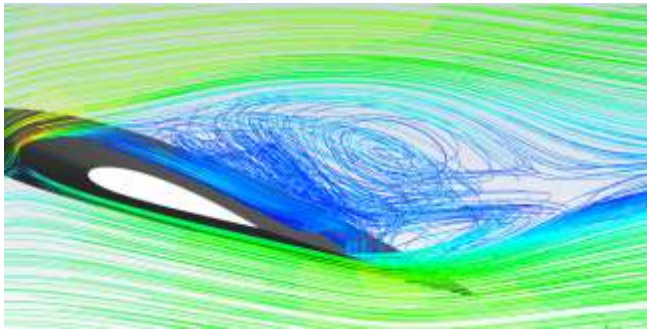

Fig- 17 : Velocity path lines @ 14deg AoA – Spanwise section (4m from root chord) view for basic wing

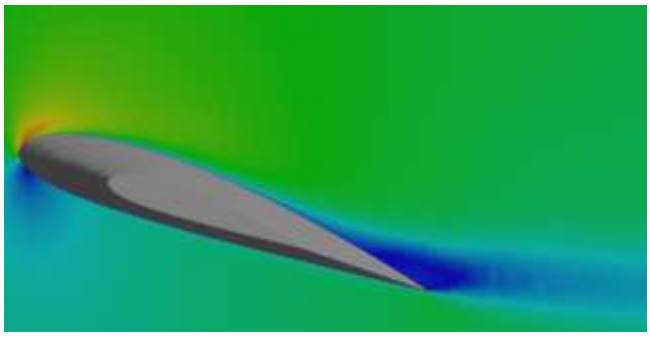

Fig- 18 : Velocity contours @ 14deg AoA – Spanwise section (4m from root chord) view for tubercle wing

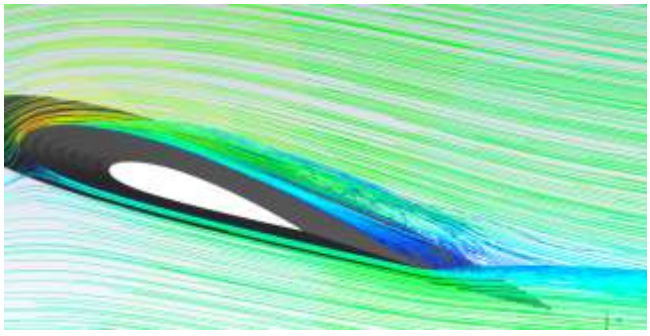

Fig- 19 : Velocity path lines @ 14deg AoA – Spanwise section (4m from root chord) view for tubercle wing

Fig-16, Fig-17, Fig-20 and Fig-21 shows the flow detachment from the wing upper surface and formation of laminar separation bubble is captured well through the sectional view of velocity streamline patterns at various 14deg and 16deg AoA for baseline and tubercle wing. Contour and streamlines are visualized span wise location at 4m and 7m respectively from the root chord. At lower angle of attack flow is fully attached over suction and pressure surface as depicted from lift curve slope.

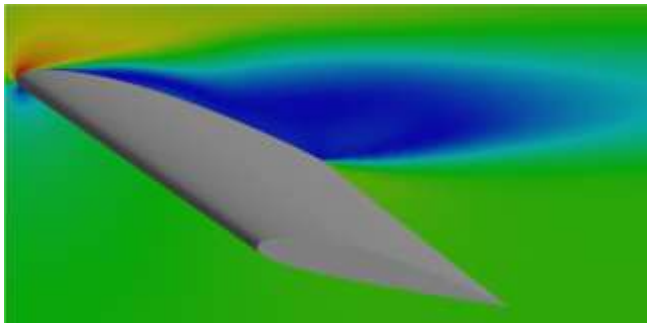

Fig- 20 : Velocity contours @ 16deg AoA – Spanwise section (4m from root chord) view for basic wing

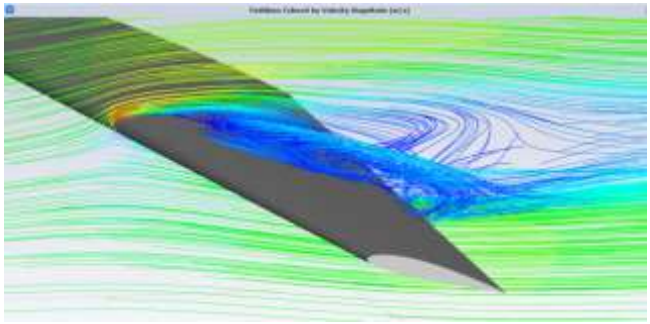

Fig- 21 : Velocity path lines @ 16deg AoA – Spanwise section (4m from root chord) view for basic wing

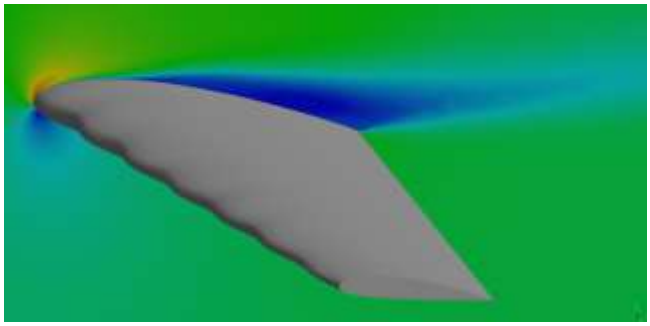

Fig- 22 : Velocity path lines @ 16deg AoA – Spanwise section (4m from root chord) view for tubercle wing

Fig-18, Fig-19, Fig-22 & Fig-23 indicates that flow separation is marginally under control for the tubercle wing profile due to presence of counter rotating vortices.

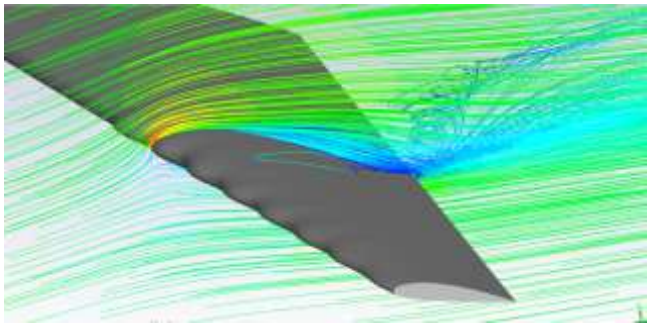

Fig- 23 : Velocity path lines @ 16deg AoA – Spanwise section (4m from root chord) view for tubercle wing

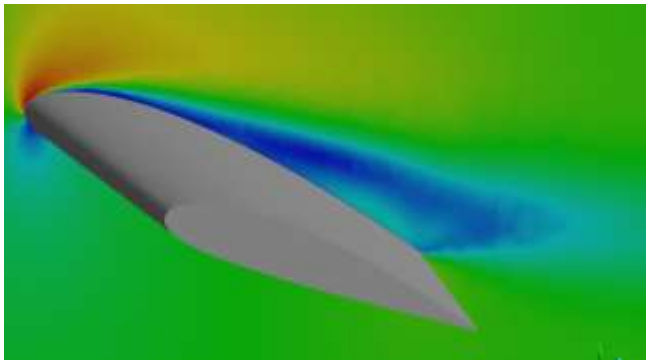

Fig- 24 : Velocity contours @ 16deg AoA – Spanwise section (7m from root chord) view for basic wing

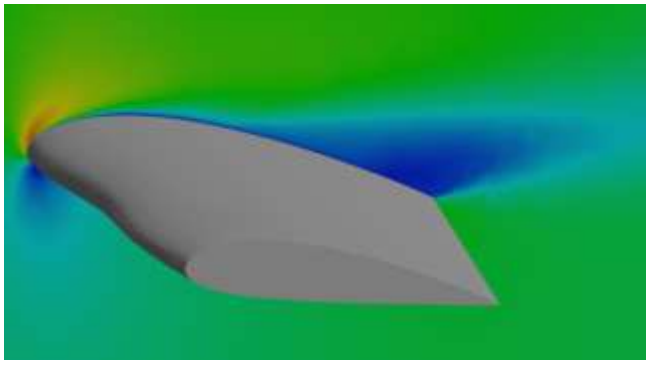

Fig- 25 : Velocity contours @ 16deg AoA – Spanwise section (7m from root chord) view for tubercle wing

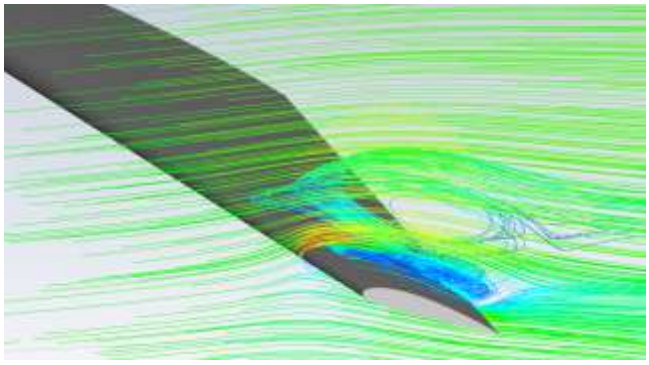

Fig- 26 : Velocity path-lines @ 16deg AoA – Spanwise section (7m from root chord) view for basic wing

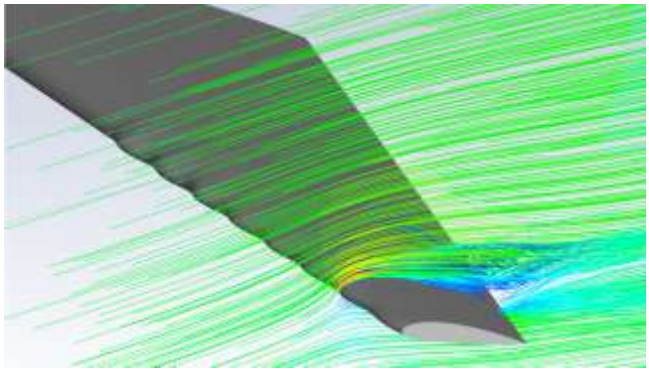

Fig- 27 : Velocity path-lines @ 16deg AoA – Spanwise section (7m from root chord) view for tubercle wing

Implementation of leading edge tubercle for the wing would replace the leading edge and trailing edge of aircraft wing to achieve the boundary layer control and delay in post stall characteristics of tubercle wings with higher aerodynamic performance (L/D) at low Reynolds number.

Fig-28 to Fig-31 shows the velocity vectors for the baseline and tubercle wing configuration. It is very clear from these figures at higher AoA huge flow separation is observed due to the adverse pressure gradients for the basic wing profile. But, for the tubercle wing profile flow remain attached even at higher angle of attack.

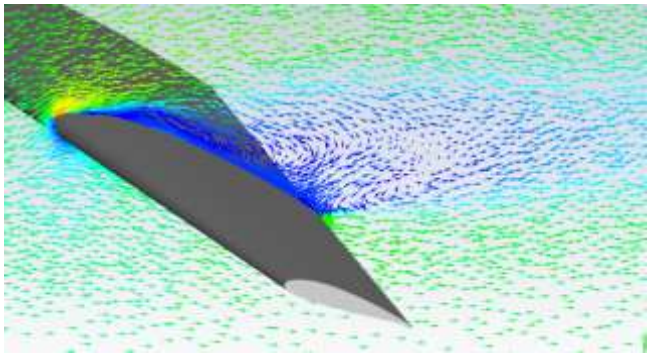

Fig- 28 : Velocity vectors @ 16deg AoA – Spanwise section (4m from root chord) view for basic wing

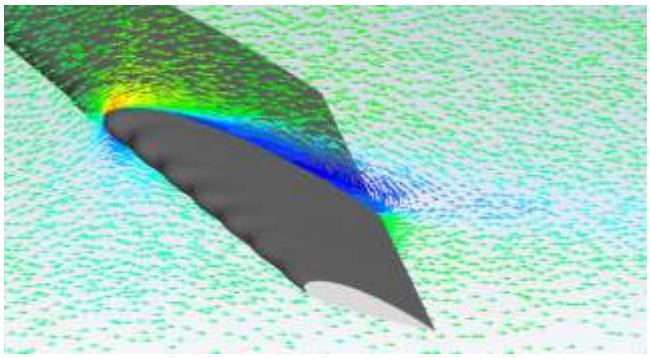

Fig- 29 : Velocity vectors @ 16deg AoA – Spanwise section (4m from root chord) view for tubercle wing

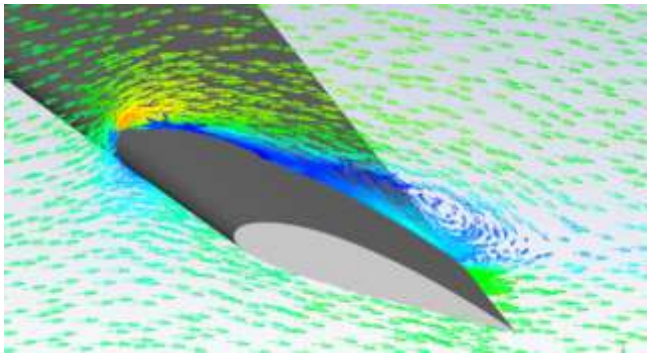

Fig- 30 : Velocity vectors @ 16deg AoA – Spanwise section (7m from root chord) view for basic wing

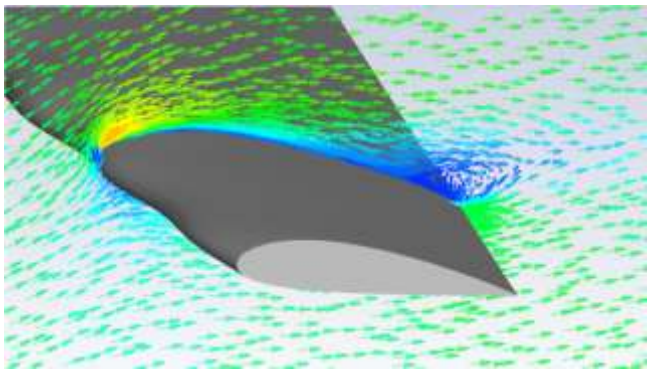

Fig- 31 : Velocity vectors @ 16deg AoA – Spanwise section (7m from root chord) view for tubercle wing

9. Conclusions

Aerodynamic performance of light jet wing has been analyzed by changing the leading edge with simple modification (tubercles) through systematic optimization of geometric parameters. CFD modeling and analysis is carried out for AoA ranging from 0deg to 16deg. It has been observed from the analysis, tubercle on the leading edge of the wing seen to have improved post stall characteristics at higher AoA by creating the counter rotating vortices in the trough region which alter the flow pattern. These counter rotating vortices could reenergize the boundary layer and keep the flow attached to the wing surface even at high angle of attack. It can be concluded that the vortices created by the tubercles cause for the delayed stall and better aerodynamic performance in the post stall region.

Nomenclature

S	Wing plan form area
c	Wing chord
C_d	Aerodynamic drag coefficient
C_l	Aerodynamic lift coefficient
C_{lmax}	Maximum lift coefficient
D	Drag force
k	Turbulent kinetic energy
L/D	Lift to drag ratio
b	Wing span
λ	Tubercle wavelength
α	angle of attack
Re	Reynolds number

REFERENCES

1. CFD study of the effect of leading-edge tubercles on the aerodynamic characteristics of a small UAV based on eppler 186 airfoils Rafael Bardera a, Angel´ Antonio Rodríguez-Sevillano b, Estela Barroso-Barderas a, Juan Carlos Matías-García. ELSEVIER Results in Engineering 23 (2024) 102639.
2. Numerical Study on the Effect of Leading Edge Tubercle on Symmetrical Airfoil at Low Reynolds Number Jeena Joseph1, A. Sathyabhama Department of Mechanical Engineering, National institute of Technology Karnataka, Surathkal, Karnataka, India Department of Mechanical Engineering, National institute of Technology Karnataka, Surathkal, Karnataka, India The International Journal of Engineering and Science (IJES)
3. Comparative Study on the Effect of Leading Edge Protuberance of Different Shapes on the Aerodynamic Performance of Two Distinct Airfoils C. Jayapal Reddy and A. Sathyabhama Department of Mechanical Engineering, NITK Surathkal, Mangalore – 575025, Karnataka, India Journal ofApplied Fluid Mechanics, Vol. 16, No. 1, pp. 157-1 77, 2023. Available online at www.jafmonline.net, ISSN 1735-3572, EISSN 1735-3645.
4. Effects of Leading-edge Tubercles on the Aerodynamic Performance of Rectangular Blades for low-speed Wind Turbine Applications Parankush Koul1*, Mahesh K. Varpe2, Pritam Bhat3, Aniket Mishra4, Chirag Malhotra5, Devang Kalra International Journal of Scientific Research in Modern Science and Technology ISSN: 2583 -7605 (Online)
5. Impact of Leading-Edge Tubercles on Airfoil Aerodynamic Performance and Flow Patterns at Different Reynolds Numbers Dian Wang, Chang Cai, Rongyu Zha, Chaoyi Peng, Xuebin Feng, Pengcheng Liang, Keqilao Meng, Energies 2024, 17, 5518. https://doi.org/10.3390/en17215518
6. Improving performances of biomimetic wings with leading-edge tubercles Giorgio Moscato1 · Jais Mohamed1 · Giovanni Paolo Romano Received: 12 April 2022 / Revised: 7 July 2022 / Accepted: 28 July 2022 / Published online: 30 August 2022 © The Author(s) 2022
7. Investigation on the effect of leading edge tubercles of sweptback wing at low reynolds number Veerapathiran Thangaraj Gopinathan1, John Bruce Ralphin Rose2,*, and Mohanram Surya
8. Numerical Investigation on the Effect of Leading-Edge Tubercles on the Laminar Separation Bubble A. Sathyabhama1† and B. K. Sreejith Journal ofApplied Fluid Mechanics, Vol. 15, No. 3, pp. 767-780, 2022.
9. Numerical Investigation of the Effect of Leading-Edge Tubercles on Propeller Performance Fa had Rafi Butt∗ and Tariq Talha Nation al Univers ity of Scienc es and Technol ogy, Rawalpin di 46000, Pakistan DOI: 10.2514/1.C034845 JOURNAL OF AIRCRAFT Vol. 56, No. 3, May–June 2019
10. Numerical Studies on the Effect of Leading Edge Tubercles on a Low-Pressure Turbine Cascade Wenhua Duan, Weijie Chen *, Xinyu Zhao and Weiyang Qiao. Energies 2023, 16, 4398. https://doi.org/10.3390/en16114398